SIMULATION OF SPACE-BORNE RADAR OBSERVATIONS OF PRECIPITATION AT KU AND KA BAND

P7.7

V. Chandrasekar * and Direk Khajonrat

Colorado State University
1373, campus Delivery
Fort Collins CO 80523-1373, USA

ABSTRACT

Global Precipitation Measurement (GPM) is poised to be the next generation precipitation observations from space after the TRMM mission. The GPM will carry a dual-frequency precipitation radar (DPR), operating at Ku and Ka band frequencies. Since space-borne precipitation observations have never been done in Ka band before, extensive research work on dual-frequency radar, including electromagnetic wave propagation characteristics from space and retrieval algorithms are essentially required in developing system design, retrievals and instrument performance evaluations. This paper presents a methodology to simulate Ku and Ka band radar observation of precipitation.

Index Terms — GPM, DPR, Simulation

1. INTRODUCTION

GPM core satellite will carry a dual frequency radar called DPR operating at two different frequencies, 13.6GHz (Ku-band) and 35.6 GHz (Ka-band) as opposed to single 13.8 GHz (Ku-band) precipitation radar (PR) on TRMM (Tropical Rainfall Measuring Mission). DPR will have two independent measurements at every range bin. By combining the two measurements, the dual-wavelength algorithms can be used to retrieve two parameters of drop size distribution (DSD) of precipitation. Using the retrieval algorithms, precipitation microphysical parameters can be estimated more accurately, which is the key improvement expected from GPM-DPR.

There are numerous assumptions in the retrieval algorithms and they are based on our current understanding of the microphysics process. One such example is the accuracy of retrieved DSD parameters using dual-wavelength algorithms relies strongly on correct identification of phase-height transition (PHT) from frozen to liquid hydrometeor along vertical profile. It is important to understand how these various features manifest themselves in dual-wavelength measurements.

Validation is an integral part of all satellite precipitation missions. During GPM era, there are going to be numerous single and dual-polarization ground radars around the globe that will be observing precipitation. It will be very useful if one could use this ground radar measurement to simulate space borne dual wavelength observations, then we have a globally diverse data set that can be used in the system design, algorithm development and validation.

This paper presents a technique to simulate GPM-DPR observations starting with single-polarization and dual-polarization radar measurements observed by ground radar.

2. REFLECTIVITY (Z) AND SPECIFIC ATTENUATION(K) RELATION AND VARIATION WITH FREQUENCY

Theoretical computation of radar reflectivity (Ze) and specific attenuation (K) were applied at three different frequencies: 2.7 GHz (S-band), 13.6 GHz (Ku-band) and 35.6 GHz (Ka-band) based on a wide variation of published precipitation size distribution (PSD) parameters and different particle density(Pruppacher and Klett ,1997; Passarelli,(1978) and Gorgucci et al. 2002). Variability of Ze with frequency for all precipitation types including snow, graupel and rain appear to be linearly related. K and Ze relations

* *Corresponding author address:* Dr. V. Chandrasekar., Colorado State University, Electrical and Computer Engineering Dept. CO. e-mail:Chandra@engr.colostate.edu

can be represented by power law relations. Figure 1 shows the K-Ze and Ze-Ze relation for dry snow particles with randomly chosen DSDs. Other particle types show similar relations as Figure 1.

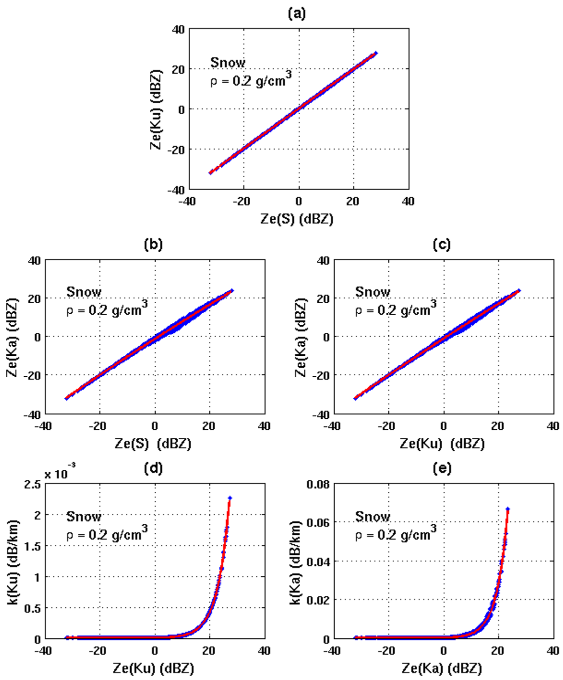

Figure 1, (a) (b) (c): Variability of Ze with frequency for S and Ku band; S and Ka band; Ku and Ka band respectively for dry snow at density 0.2g/cm^3. (d) (e): Power law relationship between k and Ze at Ku and Ka band respectively for the same hydrometeor type.

3, MICROPHYSICAL MODELS DEVELOPMENT FOR SIMULATION

Data from APR2 (second generation airborne precipitation radar) deployed in NAMMA (NASA African Monsoon Multidisciplinary Analysis) experiment in 2006 is used to study microphysical models along the vertical profiles for this simulation. APR2 is operating at Ku and Ka band which is designed to emulate GPM-DPR. Figure 2 shows an example of one overpass of NAMMA data. APR2 will provide four main measurements, namely, Zm(ku), Zm(ka), LDR (linear depolarization ratio) and fall velocity. Figure 3 and 4 shows the selected vertical profile at location A and C from Figure 2 (a).

The boundary for the ice, melting ice and rain region for a vertical profile is detected using LDR and velocity parameters. LDR>-26 dB is used as a threshold for the melting layer region for both stratiform and convective case as shown by dash line in Figure 3(c) and 4(c). Velocity has the trend to increase and then keep relatively constant during transition from ice to melting ice, and melting ice to rain region. This trend is more clear for stratiform than convective. The precipitation model for stratiform and convective are shown in Figure 5. Dual-frequency retrieval algorithm described in (Meneghini et al, 1992) is used to retrieved DSD forwardly for regions above melting layer bottom. Whereas, DSD parameters in rain region are retrieved using the same method but backwardly with the SRT (surface reference technique) calculated using DAD method described in (Iguchi, 2005).

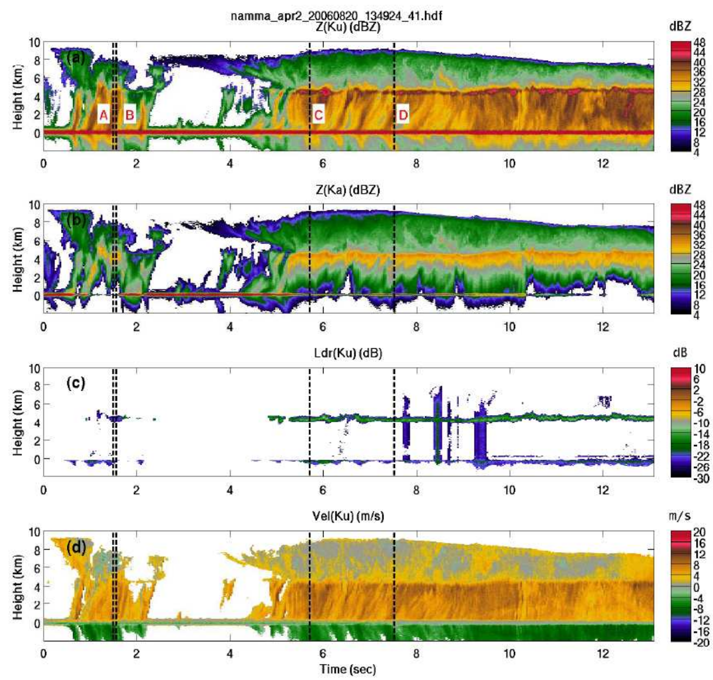

Figure 2, Overpass of NAMMA experiment data for 20060820-134924 case. (a) Zm(ku) (b) Zm(ka) (c) LDR (d) fall velocity.

A wide range of snow density is reported by a number of studies (see Liao et al, 2005; Zawadzki et al, 2005). In this case, a fixed snow density of 0.2g/cm^3 is assumed. The retrieved DSDs for stratiform profiles are shown in Figure 6. Above the bright band, the retrieved Do decreases as the height increases, while the opposite is true for log(Nw). In the bright band, the retrieved Do has a sharp decrease at the height just below the bright band peak, while the retrieved log(Nw) sharply increases accordingly. For rain region, the best fit of the retrieved Do is nearly constant along the height. Similarly, the best fit of retrieved log(Nw) is almost constant along the height, with a mild variation. The retrieval is also performed for convective case. However, the results are not presented here for brevity.

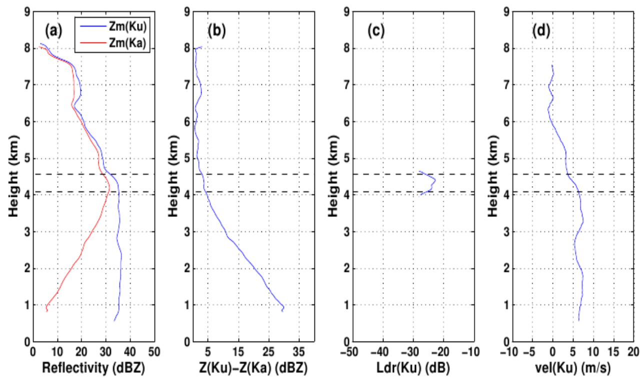

Figure 3, Picked convective profile at location A in Figure 2(a). (a) Zm(ku) & Zm(ka) ;(b) DFR(Zm(ku)-Zm(ka)); (c) LDR; (d) fall velocity.

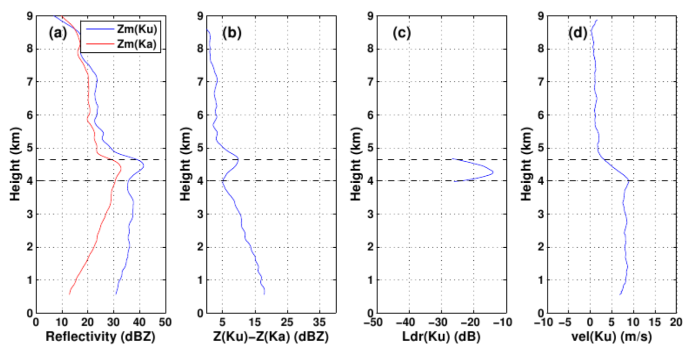

Figure 4, Picked stratiform profile at location C in Figure 2(a). (a) Zm(ku) & Zm(ka) ;(b) DFR(Zm(ku)-Zm(ka)); (c) LDR; (d) fall velocity.

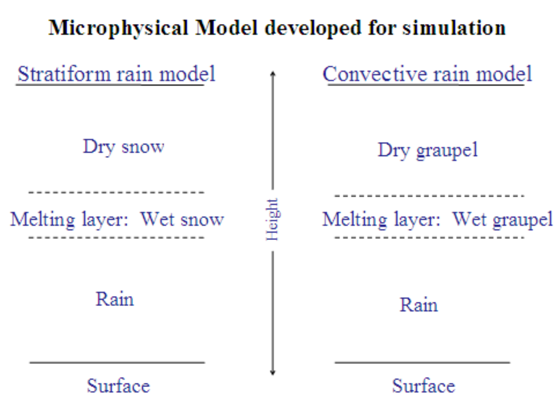

Figure 5, Scattering model developed for simulation.

4, SIMULATION OF KU AND KA BAND OBSERVATIONS USING SINGLE AND DUAL-POLARIZATION MEASUREMENTS.

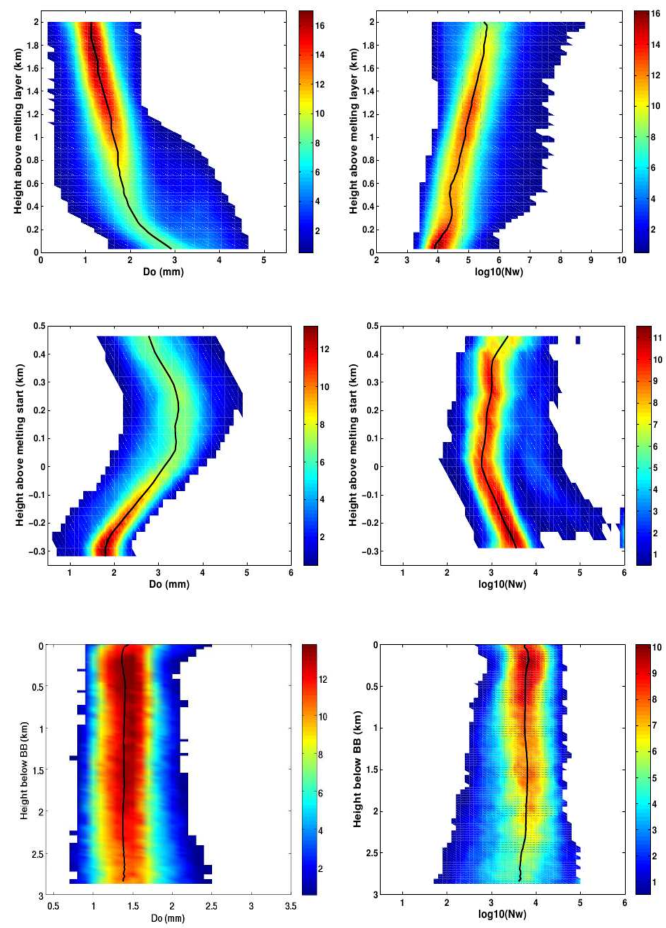

Figure 6, Retrieved DSD parameter distribution for stratiform case. Left column: retrieved Do(mm); Right column: retrieved Nw ($mm^{-1}m^{-3}$) (in log scale) . From top row to bottom: Retrieved Do or log(Nw) for regions : above bright band; within bright band; and rain.

The coefficients of parameterization between Ze and k and variability of Ze with frequency are generated at each range bin, based on the distribution of the retrieved Do and Nw of the particle type along the vertical profile for each rain type model. The generated coefficients, in a sense, are the inference of the natural variation of microphysical characteristics along the vertical profile, and will be used quantitatively for simulating Ku and Ka band observations from ground radar measurements.

4.1 A simulation using ground-based NEXRAD radar measurements.

The NEXRAD (Weather Surveillance Radar-1998 Doppler, WSR-88D or NEXRAD) is a single-polarization radar, producing two products, reflectivity and velocity. In this simulation, the reflectivity measurement from NEXRAD site, namely KTBW, located in Ruskin/Tampa Bay, FL is used. Figure 7 shows the simulated measurements of reflectivity at Ku and Ka band from a case of KTBW radar measurement on December 12, 2006.

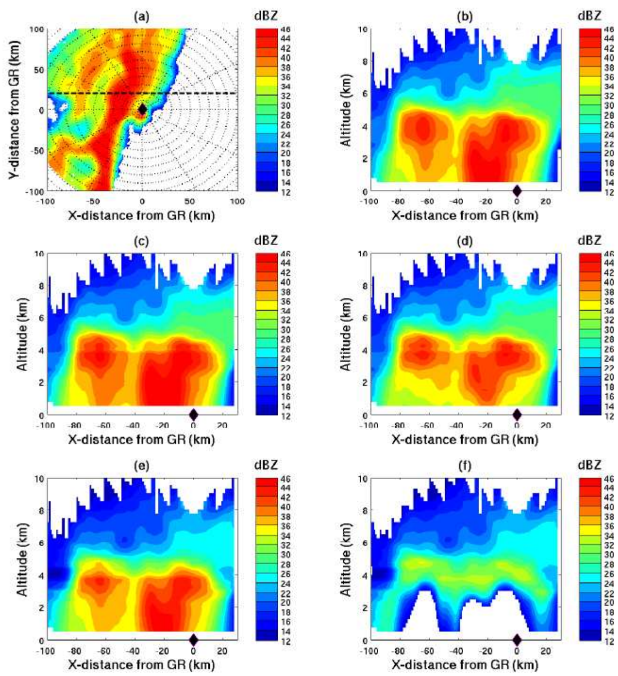

Figure 7, The vertical cross-section of reflectivity: (a) and (b) are the horizontal and vertical cross-section of Ze(S) measurement from KTBW radar, respectively; (c) and (d) are the vertical cross-section of the simulated Ze(Ku) and Zm(Ku), as indicated by the dashed line in (a), respectively; (e) and (f) are the vertical cross-section of the simulated Ze(Ka) and Zm(Ka), respectively.

From Figure 7 (b) and (c), the vertical cross-sections look similar. This is because of the Rayleigh scattering which dominantly occurs in both channels. On the other hand, (e) shows several dBZ lower than (b). This is caused by non-Rayleigh scattering in the Ka band and Rayleigh scattering in S band. It is clear that in (f), the attenuation causes the loss of signal in Ka band at an altitude up to 2km above the surface. Since there is no rain type information available from KTBW, the rain type classification method (H- and V-method) (Awaka et al,1997) is used here to classify stratiform and convective type. Due to the coarse vertical resolution of the ground radar observations, melting layer region detection could only be roughly detected for NEXRAD case.

4.2, A simulation using dual-polarization ground-radar measurements.

The key feature of the simulation of DPR observations using dual-polarization ground-based radar measurements is that the phase-height transition (PHT) of precipitation particles, which is very important in the simulation, can be obtained via dual-polarization measurements. (Lim and Chandrasekar, 2005) have shown that the fuzzy logic techniques using dual-polarimetric measurements provide a promising result for hydrometeor classification

Dual-polarization radar measurements were obtained from CSU-CHILL radar during a severe thunderstorm electrification and precipitation study (STEPS) project in 2000. Figure 8 shows the horizontal and vertical cross-sections of the reflectivity and the fuzzy hydrometeor classification results.

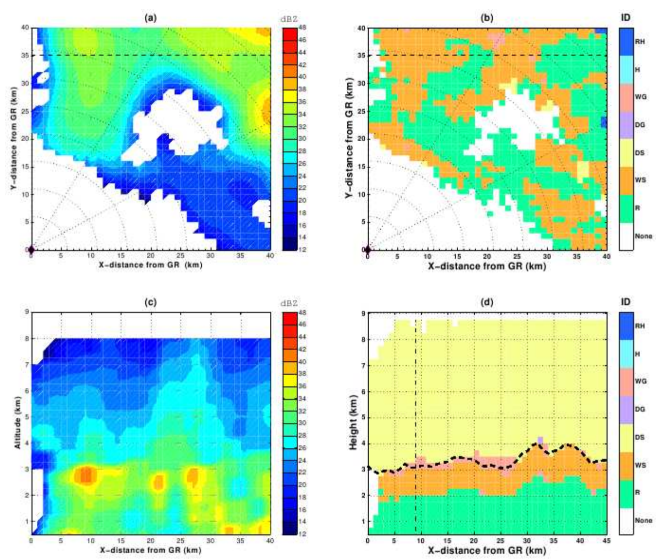

Figure 8, (a) The horizontal cross-section of reflectivity;(b) the horizontal cross-section of reflectivity particle type from fuzzy classification results; (c) the vertical cross-section of reflectivity , as indicated by the dashed line in (a); (d) the vertical cross-section of particle type from fuzzy classification results, as indicated by the dashed line in (b).

The simulation is performed along the vertical profile corresponding to the results of hydrometeor classification. Figure 9 (a) shows a vertical cross-section of the hydrometeor classification results (same as Figure 8(d)). Three dual-polarization measurements, LDR, ρ_{hv} and Zdr are shown in Figure 9 (b). It can be seen that the melting layer signatures of LDR, ρ_{hv} and Zdr are apparent. A vertical profile is selected, as indicated by the dashed line in Figure 9(a), for a demonstration of the simulation.

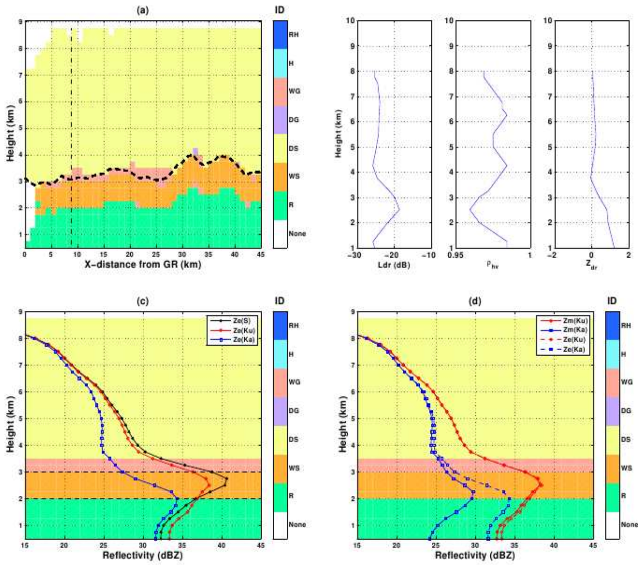

Figure 9, (a) The vertical cross-section of hydrometeor type; (b) the vertical profiles of three polarimetric measurements, namely, LDR, ρ_{hv} and Zdr; (c) the vertical profile of Ze(S), the simulated Ze(Ku), and Ze(Ka) , as indicated by the dashed line in (a); (d) the vertical profile of the simulated Ze(Ku), Zm(Ku), Ze(Ka), and Zm(Ka).

Figure 9(c) shows the vertical profile of Ze(S), the simulated Ze(Ku) and the simulated Ze(Ka) along with the vertical profile of precipitation particles that reflect their phase-height transitions. In this case, the profile is stratiform rain with a bright band around 1km. The height of the bright band from the ground and its thickness agree well with the three polarimetric measurements. Note that the bright band peak in this case is quite low when compared with the data from NEXRAD radar. This is because of the measurements were taken in Colorado, a relatively high latitude precipitation regime, even though it was in a summer. In (d), it can be seen that there is no attenuation in dry snow region in Ku band, whereas a small attenuation about 1dB is observed in Ka band. In the bright band, the attenuation is found to be about 5dB in Ka band and a fraction of dB in Ku band. Since the rain region of the profile is only 2 km above the ground, even though there is an intense convective rain, a strong attenuation by rain is unlikely to cause an extinction of the signal. Therefore, dual-frequency retrieval algorithms are always applicable for this precipitation regime.

5, SUMMARY

Simulation of Ku and Ka band observations were performed using single- and dual-polarization ground based radar measurements. Airborne dual-frequency radar observations from NAMMA experiment were used to develop the simulation models. The simulation results show that path integrated attenuation at Ka band PIA(Ka) is almost 10 times PIA(Ku).

The phase-height transition can be determined quite accurately when using dual-polarization radar measurements. For the case studied, the simulation results suggest that the dual-frequency retrieval algorithms were always applicable because of the short rain column. This paper presents a quantitative Ku and Ka band simulation based study that will be useful for designing GPM-DPR system and examine retrievals.

ACKNOWLEDGMENT

This research is supported by the NASA GPM/PMM program.

REFERENCES

Awaka, J., T. Iguchi, H. Kumagai, and K. Okamoto, 1997: Rain type classification algorithm for TRMM precipitation radar. *Proc. IEEE IGARSS'97*, 317-319.

Gorgucci, E., G. Scarchilli, V. Chandrasekar, and V. Bringi, 2002: Estimation of rain-drop size distribution parameters from polarimetric radar measurement. *J. Atmos. Sci.,* 59(15), 2373-2384.

Iguchi, T, 2005 :Possible algorithm for the dual-polarization precipitation radar (DPR) on the GPM core satellite. *32nd Conf. on Radar Meteorology, Amer. Meteor. Soc.,* Albuquerque, NM, CD-ROM.

Liao, L., R. Meneghini, T. Iguchi, and A. Detwiler, 2005: Use of dual-wavelength radar for snow parameter estimates. *J.Atmos. Oceanic Technol*., 22, 1494-1506.

Lim, S. and V. Chandrasekar, 2005: Hydrometeor classification system using dual-polarization radar measurement: Model improvement and in situ verification. *IEEE Trans. Geosci. Remote Sens.* 43(4), 792-801.

Meneghini, R., T. Kozu, H. Kumagai, and W. C. Boncyk, 1992: A study of rain estimation methods from space using dual-wavelength radar measurements at near nadir incidence over ocean, *J. Atmos. Ocean. Technol.,* vol. 9, pp. 364-382.

Passarelli, R. E., 1978: Theoretical and observation study of snow-size spectra and snowflake aggregation efficiencies. *J. Atmos. Sci*., 35, 882-889.

Pruppacher, H. R. and J.D. Klett, 1997: Microphysics of Clouds and Precipitation. 2nd ed.

Zawadzki, I., W. Szyrmer, C. Bell, and F. Fabry, 2005: Modeling of the melting layer. Part III: The density effect. *J. Atmos. Sci*., 62, 3702-3723.